

NEW CONCEPT FOR A CLIC POST-COLLISION EXTRACTION LINE

A. Ferrari*, Uppsala University, Sweden

Abstract

Strong beam-beam effects at the interaction point of a high-energy e^+e^- linear collider such as CLIC lead to an emittance growth for the outgoing beams, as well as to the production of beamstrahlung photons and e^+e^- coherent pairs. We present a conceptual design of the post-collision line for CLIC at 3 TeV, which separates the various components of the outgoing beam in a vertical magnetic chicane and then transports them to their respective dump.

INTRODUCTION

The Compact Linear Collider (CLIC) study aims at multi-TeV e^+e^- collisions with the two-beam acceleration technology [1]. In order to achieve high charge densities and, in turn, to reach the desired luminosity, the incoming beams must be focused to extremely small spot sizes. As a result, they experience very strong electromagnetic fields at the interaction point. The bending of their trajectories then leads to the emission of beamstrahlung photons, which can then turn into e^+e^- coherent pairs. A careful design of the post-collision line must be performed in order to transport the charged particles and the beamstrahlung photons from the interaction point to the dump with small losses. We propose a design based on the separation of the disrupted beam, the beamstrahlung photons and the coherent pairs just after the interaction point, followed by a transport to the dump through dedicated extraction lines. Key CLIC parameters like the RF frequency, the accelerating gradient and the bunch charge have recently been modified. In this study, we still consider the incoming beam parameters of Ref. [2], see Table 1.

INCOMING AND OUTGOING BEAMS AT THE INTERACTION POINT

The upper plot of Figure 1 shows the angular distributions of the disrupted beams. The double-peak shape of the x' distribution is characteristic for collisions with flat beams. Strong beam-beam interactions lead to an increase of the angular divergence. The energy spectrum after the bunch crossing is shown in the lower plot of Figure 1. The long low-energy tail results from the emission of photons (in average 1.1 per incoming electron or positron). The corresponding average energy loss of each incoming beam is 16%. The horizontal and vertical rms opening angles of the beamstrahlung photon cone are respectively $33 \mu\text{rad}$ and $26 \mu\text{rad}$. Finally, one expects 4.6×10^7 coherent pairs per bunch crossing at CLIC. Their electrons and positrons carry typically about 10% of the primary beam energy.

Table 1: Incoming beam parameters at the interaction point of the CLIC machine.

| Parameter | Symbol | Value |
|----------------------|-------------------------------|--|
| Beam energy | E | 1.5 TeV |
| Particles per bunch | N_b | $2.56 \cdot 10^9$ |
| Bunches per RF pulse | n | 220 |
| Bunch spacing | Δt_b | 0.267 ns |
| Repetition frequency | f | 150 Hz |
| Primary beam power | P_b | 20.4 MW |
| H/V emittances | $(\beta\gamma)\epsilon_{x,y}$ | 660, 10 nm.rad |
| H/V rms beam sizes | $\sigma_{x,y}$ | 60, 0.7 nm |
| Rms bunch length | σ_z | $30.8 \mu\text{m}$ |
| Peak luminosity | L | $6.5 \cdot 10^{34} \text{ cm}^{-2} \text{ s}^{-1}$ |

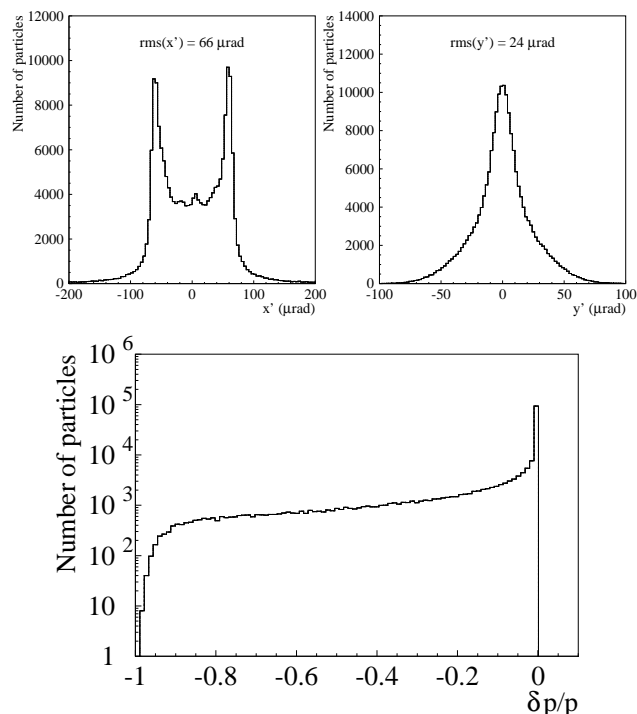


Figure 1: Angular distributions and energy spectrum of the CLIC disrupted beam at the interaction point.

EXTRACTION AND SEPARATION OF THE OUTGOING BEAMS

Our design is based on the separation of the disrupted beam, the beamstrahlung photons and the e^+e^- coherent pairs by a magnetic chicane, just after the interaction point, see Figure 2.

* ferrari@tsl.uu.se

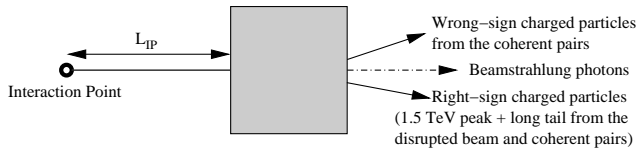


Figure 2: Schematic layout of the separation of the three components of the outgoing beam just after the interaction point, while they are still inside a common vacuum pipe.

The optimal crossing angle at CLIC is 20 mrad [3]. Due to the presence of the incoming beam line, some compact vertical bending magnets must be used. In our design, the various components of the outgoing beam are separated by using four window-frame magnets. The distance between the interaction point and the entrance of the first extraction magnet is 16 m, which ensures that it is placed outside the detector. With a field strength of 1 T and a length of 4 m each, the four extraction magnets provide a total bending angle of 3.2 mrad at 1.5 TeV.

The transverse beam sizes were carefully estimated at the entrance and exit of each magnet, in order to derive the adequate sizes for the vacuum pipe in the air gaps, and thereby for the dipoles themselves. Particle trackings were performed with DIMAD [4] for this purpose. One way to have simultaneously small power losses and reasonable magnet dimensions is to install collimators in the 1 m long drift spaces between two consecutive dipoles. By absorbing the charged particles with an energy deviation $\delta < -0.95$, these collimators make sure that the beam transport in the extraction magnets is practically loss free.

Just after the fourth extraction magnet, we physically separate the particles of the coherent pairs with the wrong-sign charge from the other components of the outgoing beam, see Figure 3.

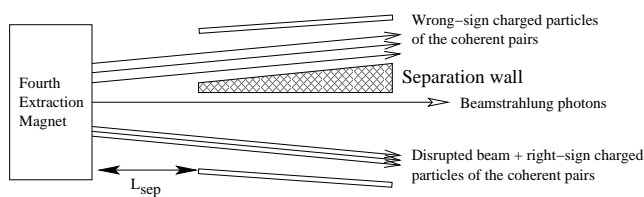


Figure 3: Schematic layout of the separation region, just downstream of the fourth extraction dipole magnet.

With $L_{sep} = 3$ m, the vertical dispersion (and thus the distance between the centre of the beamstrahlung photon cone and the 1.5 TeV reference wrong-sign charged particle of the coherent pairs) is large enough to allow insertion of a 5 mm thick wall where the separation occurs.

Following their physical separation from the other beam components, the particles of the coherent pairs with the wrong-sign charge are immediately brought to their dump. The energy spectrum of the coherent pairs is derived from the vertical distribution of the wrong-sign charged beam, before it becomes too large to fit inside a vacuum pipe with

reasonable dimensions (the other particles of the coherent pairs can not be distinguished from the low-energy tail of the disrupted beam). The left-hand side plot of Figure 4 shows the correlation between the vertical position and the energy of the particles of the coherent pairs with the wrong-sign charge, just after the separation region. On the right-hand side plot, a comparison between the energy spectrum derived from the vertical beam profile and the true one is presented: a good agreement is obtained and almost the whole energy distribution of the e^+e^- coherent pairs can be retrieved with this method.

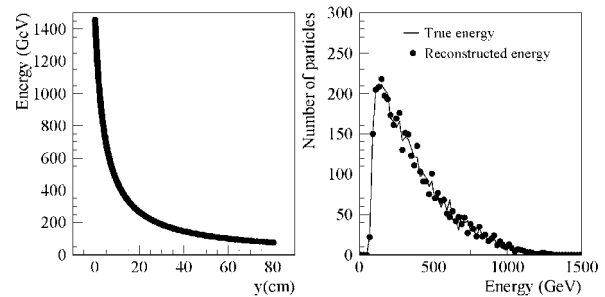


Figure 4: Reconstruction of the energy spectrum of the e^+e^- coherent pairs from the vertical beam profile of the wrong-sign charged particles after the separation region.

TRANSPORT OF THE DISRUPTED BEAM AND THE BEAMSTRAHLUNG PHOTONS

The method used to rapidly collect the wrong-sign charged particles of the coherent pairs after the separation region can not be used for the transport line of the other main charged beam. One needs the exit window to be further away from the interaction point (250 m typically), so that the transverse sizes of the non-colliding beam are large enough not to damage the window via a high local energy deposition. On the other hand, a long drift space with no magnetic element between the separation region and the dump is not a solution either, as it would rapidly lead to a very large disrupted beam. Hence, the bend provided by the four extraction magnets should be followed by a bend in the opposite direction, in order to eventually have $D'_y = 0$ downstream of the vertical chicane.

For this purpose, we propose to use four C-type dipole magnets, each with a length of 4 m and a field strength of 0.973 T (in order to compensate for the energy loss due to synchrotron radiation). They are placed after the dump of the wrong-sign charged particles of the coherent pairs to avoid encumbrance problems. All beamstrahlung photons and all charged particles with $\delta > -0.85$ pass through the vertical chicane and reach the dump. The lost particles are absorbed in five collimators placed between the separation region and the first C-type magnet. A schematic layout of this first section of the transport line for the disrupted beam is shown in Figure 5.

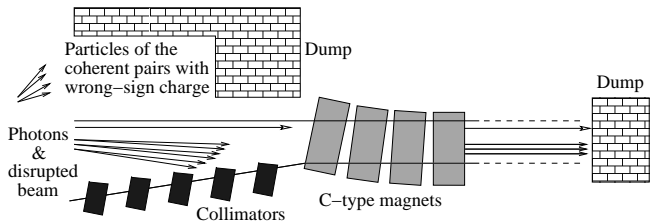


Figure 5: Schematic layout of the second part of the vertical chicane, which bends back the disrupted beam and the particles of the coherent pairs with the same charge, thus ensuring that D'_y vanishes after the last C-type magnet.

At the exit of the chicane, the low-energy particles of the disrupted beam still have $y' < 0$. In order to avoid beam losses, without significantly increasing the transverse apertures of the vacuum pipe (and thereby the size of the dump window, which could yield a too large mechanical stress), one solution is to bend back the low-energy particles which are far away from the high-energy peak, with $y' < 0$. Meanwhile, the core of the charged beam should remain unaffected. For this purpose, we use 16 vertically focusing quadrupoles centered on the path of the high-energy peak of the disrupted beam. Here, each quadrupole has a length of 2 m, a pole field of 1 T, and an aperture radius of 70 cm. Two consecutive quadrupoles are spaced by 1 m, the first one being installed 150 m after the interaction point.

Figure 6 shows the y and y' distributions of the disrupted beam as a function of the energy, at the exit of the last quadrupole (197 m downstream of the interaction point).

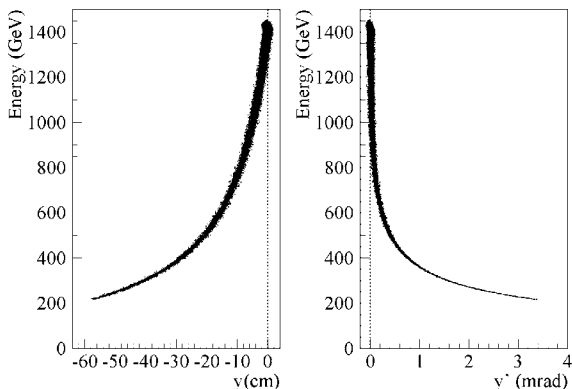


Figure 6: y and y' distributions as a function of the energy for the disrupted beam, just after the vertically refocusing region.

The presence of a refocusing region allows flexibility in the design of the last section of the CLIC post-collision line, including the dump window, because the vertical size of the disrupted beam decreases with the distance from the interaction point to the dump. Figure 7 shows the beam profiles at the dump window, located 50 m downstream of the last quadrupole in the present design.

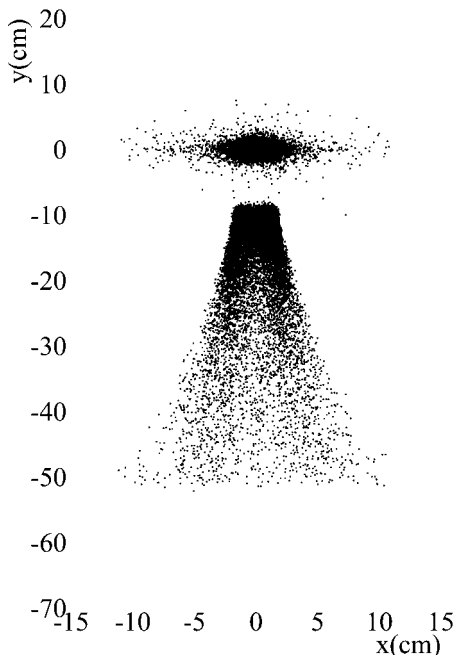


Figure 7: Transverse beam profiles obtained at the dump window, 247 m downstream of the interaction point.

CONCLUSION

A new design of the CLIC post-collision extraction line was presented in this paper, based on DIMAD particle trackings in the case of ideal e^+e^- collisions.

In a more detailed study [5], we also showed that the performance of this post-collision line is not significantly affected by small vertical beam-beam offsets in position and/or angle at the interaction point. These offsets have an influence on the disruption process and can be identified by measuring the displacement and/or distortion of all components of the outgoing beam. They may also lead to additional losses along the post-collision line, however these will only occur in the collimators.

ACKNOWLEDGEMENTS

This work is supported by the Commission of the European Communities under the 6th Framework Programme "Structuring the European Research Area", with contract number RIDS-011899.

REFERENCES

- [1] I. Wilson, Phys. Rep. 403-404 (2004) 365-378.
- [2] F. Tecker *et al.*, CLIC note 627.
- [3] D. Schulte and F. Zimmermann, CLIC note 484, presented at PAC'01, Chicago, USA.
- [4] <http://www.slac.stanford.edu/accel/ilc/codes/dimad>
- [5] A. Ferrari, EUROTeV-Report-2007-001, CLIC note 704.